Mitt. Ges. Geol. Bergbaustud. Österr. 41, Wien 1996, 45-52

Rollover and hanging-wall collapse during Sarmatian/Pannonian synsedimentary extension in the Eisenstadt Basin

Kurt Decker and Herwig Peresson

Institut für Geologie, Geo-Zentrum der Universität Wien
Althanstraße 14, A-1090 Wien

ABSTRACT

Miocene synsedimentary extensional tectonics along a listric WNW-dipping fault which formed the eastern boundary of the Eisenstadt Basin resulted in the deposition of Sarmatian/Pannonian growth strata, in the formation of a pornounced rollover anticline, and in the collapse of the hanging-wall during its adaption to the geometry of the normal fault. Excellent outcrop conditions in a gravel pit S of St. Margarethen (Burgenland) allow to evaluate the relative importance of vertical simple shear, simple shear along planes dipping antitethically to the listric fault, and fault-bend folding during the formation of the rollover.

The mesoscale faults mapped in the sandpit and the low finite strain estimated for these faults indicate that mesoscale faulting was of minor importance for the formation of rollover. Significant offsets were only recorded for normal faults which dip syntethically to the listric master fault. Antitethic faults accomodated much less than 1 % extensional strain and did not contribute to the evolution of the observed growth strata- and rollover geometry.

Observations in growth-strata conglomerates show that some deformation occured by pressure solution and extensional fracturing of pebbles. Such microscale structures indicate the predominance of coaxial pure-shear related to compaction and horizontal extension parallel to the dip direction of normal faults. Microscale shear fractures oriented antitethically to the listric master fault are less important. The importance of distributed simple-shear by movement along grain boundaries was estimated to be low by evaluating the geometries of early-formed conjugate normal faults which were rotated during rollover formation. Comparison of the observed fault geometries to deformation patterns which were modelled for vertical simple shear, antitethic simple shear and fault-bend folding shows that the observed geometries of rotated conjugate faults cannot be acchieved by distributed simple shear. It is concluded, that the rollover at the eastern boundary of the Eisenstadt Basin dominantely formed by fault-bend folding and that simple shear was not important for hanging-wall collapse.

Key words: extension tectonics, rollover, growth strata, Miocene, Eisenstadt Basin

Introduction

In the past years several papers have evaluated the relative importance of normal fault geometry, the direction of relative particle motion during the hanging-wall collapse, and the effects of sedimentation and compaction for the formation of rollover and growth strata depostition (Groshong, 1989; Rowan and Klingfield, 1989; White et al., 1986; Xiao and Suppe, 1989; 1992). Several mechanisms have been proposed which can account for the deformation in the hanging-wall during movement along a curved normal fault (Fig. 1). Vertical collapse models proposed downward motion of particles in the hanging-wall by simple-shear parallel to vertical planes to fill the opening space between the moving hanging-wall and the listric fault plane (Fig. 1-1; e.g., White et al., 1986). The more widley accepted inclined shear models assume that particles move along arbitrarily inclined shear planes which dip antitethically to the listric fault (e.g., White and Yielding, 1991).Shear along planes which are inclined with about 65°-70° and which parallel antitethic normal faults has been prefered by some authors (Fig. 1-2, Coulomb collapse; Xiao and Suppe, 1989; 1992). However, analyses of particle paths by analogue modelling have shown that the displacement field in the hanging-wall is inhomogenous and that collapse cannont be described by only

one direction of simple shear (Ellis and McClay, 1988). These simple shear models compete with modls in which adaption of the hanging-wall to the listric fault geometry occurs by fault-bend folding associated with slip along bedding planes (Fig. 1-3; Xiao and Suppe, 1992). The correct evaluation of the mechanism of hanging-wall collapse of fundamental importance in cross-section balancing. It has been shown that different assumptions made by balancing techniques lead to markedly different results for the down-dip projection of listric normal faults and for estimates of finite extension values (Rowan and Klingfield, 1989; White et al., 1986). In particular, the balancing results are very sensitive to the direction of simple shear assumed for deformation of the hanging-wall block.

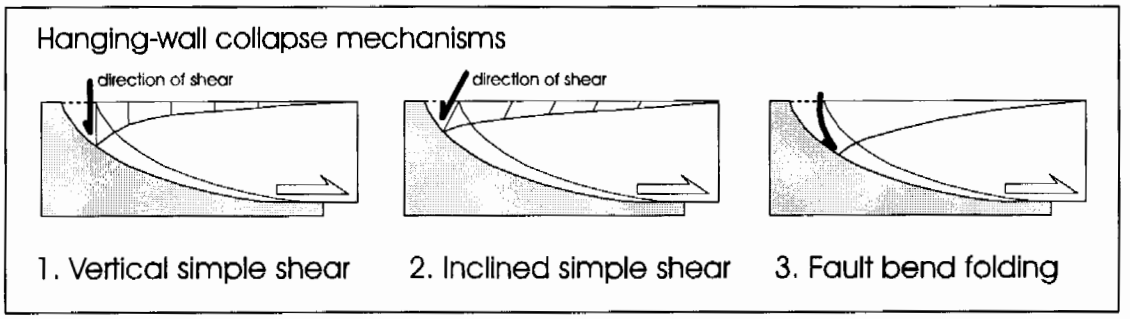

Fig. 1. Diagrams to illustrate possible mechanisms of hangingwall collapse during slip along a listric normal fault. The potential void beneath the hanging wall can be closed by (1) simple shear along vertical planes, (2) by simple shear in the direction of antitethic normal faulting, and (3) by fault bend folding.

Rollover during hanging-wall collapse in response to slip on listric normal faults during concurrent sedimentation is a widespread feature in the extensional basins at the eastern margin of the Eastern Alps. Prominent rollovers and growth strata geometries are depicted in seismic sections from the Vienna Basin (e.g., from formations adjacent to the Steinberg- and Bockfließ fault system, Wessely, 1993; OMV Exploration Group, pers. comm.), and the Eisenstadt Basin. In the Eisenstadt Basin, 12 km SSE of Eisenstadt, a rollover with growth strata of Sarmatian/Pannonian age are exposed in a gravel pit south of St. Margareten (Fig. 2). This excellent outcrop allows very detailed mapping of the growth strata geometry and of the small-scale deformational structures within the hanging-wall. The results allow an evaluation of deformation mechanisms during hanging-wall collapse and favour the fault-bend folding model for the St. Margarethen rollover.

Tectonic setting

The Eisenstadt Basin is located at the transition of the Eastern Alps to the Pannonian Basin system, close to the Austrian-Hungarian border. Miocene sediments unconformably overly crystalline basement units and Triassic low-grade metamorphic sediments of the Lower Austroalpine nappe complex (Fig. 2). Sediments include Ottnangian to Karpathian limnic and fluviatile sequences, Badenian shallow-water limestones (Leithakalk Fm.) and marine basinal marls, and Sarmatian to Pannonian clastic sequences which recorded the transition from marine to brackish conditions during the Late Sarmatian (Tollmann, 1955; Fuchs, 1965; Lueger, 1980; Tollmann, 1985). The up to 2.2 km deep basin is confined by two NE-SW and N-S trending basement highs which separate it from the Vienna Basin to the NW and from the Pannonian Basin to the E (see maps by Kröll and Wessely, 1993). Tectonic maps depict distinctly NE-SW and N-S-striking normal faults which parallel these basement highs (Tollmann, 1985; Kröll and Wessely, 1993). The eastern boundary fault parallels the N-S trending Rust mountains (Fig. 2). In the footwall of this W-dipping normal fault crystalline basement rocks, transgressively overlying Karpatian gravels (Rust Fm.),

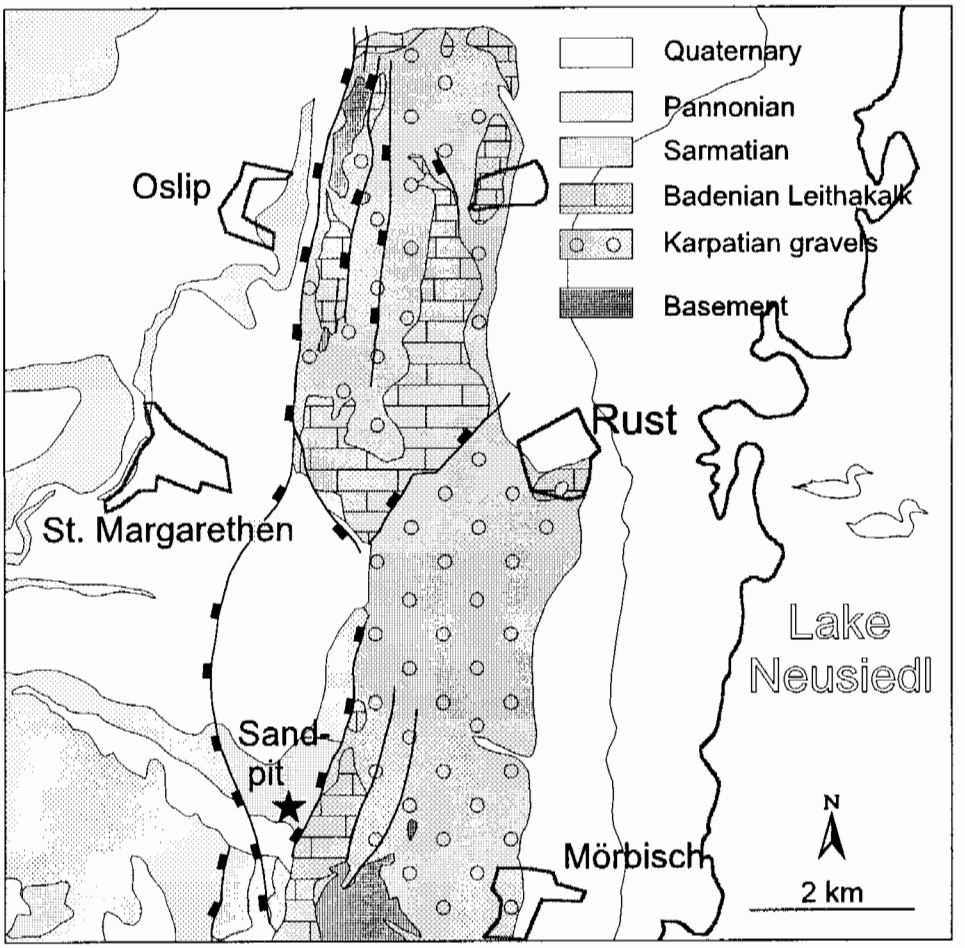

Fig. 2. Geological map of the eastern part of the Eisenstadt Basin redrawn from the Geological Map of Austria 1 : 50.000, No. 78, Rust (Hermann et al., 1993). The sandpit SSE of St. Margarethen is located close to a major NNE-striking normal fault forming the western margin of the Rust mountains.

and Badenian limestones (Leithakalk Fm.) crop out. In the hangingwall, Sarmatian and Pannonian clastics are exposed in a sand- and gravel pit south of St. Margarethen (Piller and Vávra, 1991; Piller et al., 1996). These strata show spectacular rollover and growth strata geometries which indicate synsedimentary Sarmatian-Pannonian normal slip along the WNW-dipping listric normal fault which, according to geological mapping, crops out some 100 m E of the sandpit. There, the fault forms the boundary between Pannonian strata exposed in the sandpit and Badenian limestones of the Leithakalk Formation.

Rollover and growth strata geometries

The sedimentary sequence which is exposed in the gravel pit St. Margarethen-Gemeindewald consists of interlayerd medium- to coarse-grained, cross-bedded sandy conglomerates, fine-grained silty sand and silt. Except for some bioclastic carbonate sandstones, lithification and cementation is very poor throughout the section.

The sequence forms a rollover anticline which is exposed in the northern and southern walls of the sandpit. The axis of the anticline dips 044/04, parallel to the strike of the exposed normal faults (Fig. 3). The axial trend, however, deviates from the mapped master fault which strikes NNE. Within the scale of

the quarry, bedding planes depict a fan-shape pattern typical for growth strata with bed thicknesses regularly increasing from W to E. An increase of thickness of about 75 % (from 6,5 m to 11,5 m apparent thickness) within a horizontal distance of only 50 m has been measured for a group of beds in the southern wall (Fig. 3). These unit includes a 1.5 m thick sandbed which pinches out over a distance of 20 m. Dip of the bedding planes increases both from W to E and from the higher stratigraphic level to the lowermost exposed beds. The dip of the lowermost exposed beds regularely increases over a distance of 120 m from less than 10° in the western part of the pit to 43° in its eastern part.

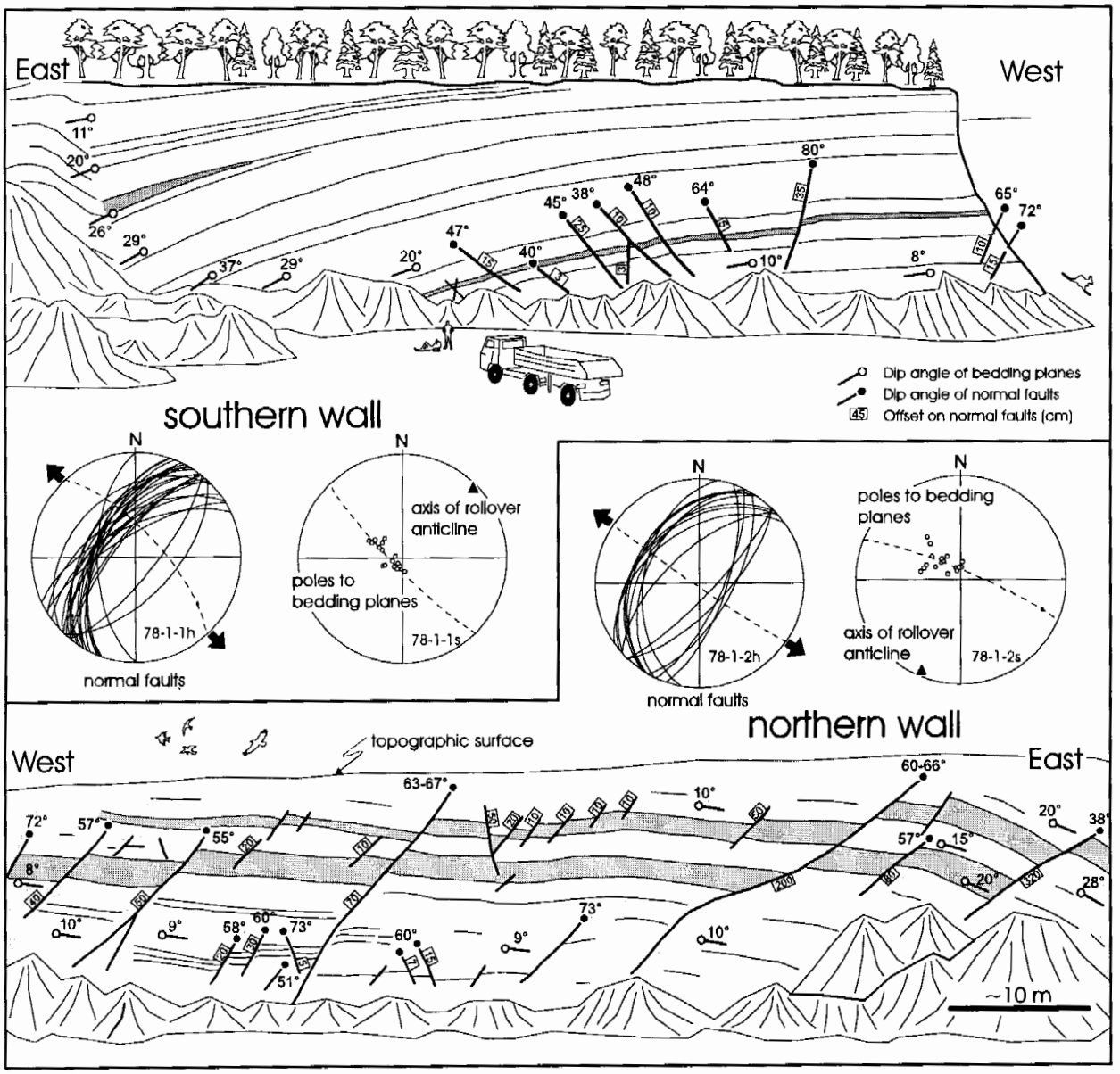

Fig. 3. Sketch of the rollover in the gravel pit St. Margarethen-Gemeindewald (see Fig. 2 for location). The Sarmatian/Pannonian growth strata form a rollover anticline with a NE-SW trending axis which parallels the strike of exposed normal faults. The rollover formed above a listric ENE-dipping normal fault which crops out E of the quarry. Bed thicknesses of the growth strata regularely increase from W to E. Strata dip towards the master fault with dip angles steepening from W to E. The normal exposed faults strike parallel to the rollover anticline. NE-dipping faults which are oriented syntethically to the master fault dominate over antitethic normal faults which are less frequent and show lower displacements. Many of the faults terminate upsection indicating synsedimentary faulting during the formation of rollover and hanging-wall collapse. Plots of normal faults and poles to bedding planes are lower hemisphere Schmidt projection.

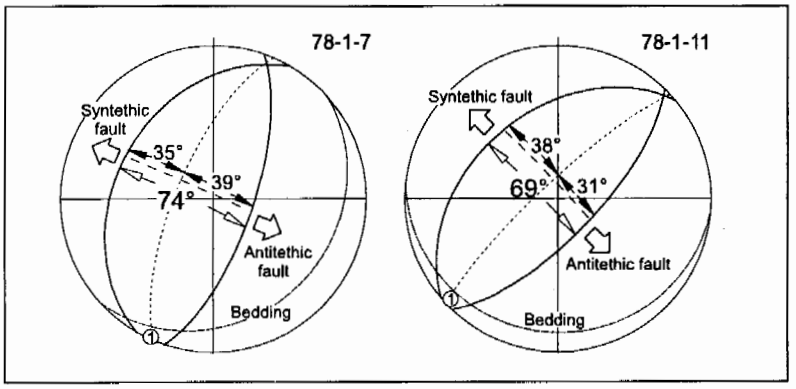

Fig. 4. Sets of conjugate normal faults measured in the rollover (see Fig. 4). Full great circles: normal faults; dashed great circles: bedding planes and reference planes oriented perpendicular to bedding. Fault orientations are nearly symmetrical with respect to the bedding plane (reference plane) indicating faulting in horizontally bedded strata and rotation of the faults during the formation of rollover.

Deformational structures

Mesoscale fault patterns

The northern and southern wall of the pit expose arrays of mesoscale NW- and SE-dipping normal faults (Fig. 3). The NW-dipping normal faults which dip syntethically to the master fault which was mapped about 100 m E of the outcrop (Fig. 2) dominate over SE-dipping antitethical faults. Syntethic faults are more frequent and show longer outcrop traces and larger offsets. In the northern wall, NW-dipping faults which can be traced throughout the exposed sequence occur at a regular spacing of about 20 m. Fault dips which vary between 65° and 40° show a tendency to decrease from W to E, indicating that the normal faults in the easternmost part of the sandpit were rotated during rollover formation. The vertical throws vary between 0.5 to 3.2 m. In between these larger-scale faults, a number of minor faults occurs which can only be traced through the section for several meters and which display normal offsets up to 30 cm. Many of these small-scale faults terminate upsection in sandy conglomerates. NW-dipping faults syntethic to the master fault of the rollover are significantly more abundant than conjugate SE-dipping faults. The few SE-dipping antitethic faults observed dip more steeply than the syntethic faults, again arguing for rotation during rollover formation. Most of the SE-dipping faults display offsets of only few centimeters. Fault patterns in the rollover of the southern wall of the pit are again strongly dominated by NW-dipping faults. All observed faults terminate upsection within the inclined beds of the rollover indicating that faulting occured synsedimentarily and synchronously with the rollover formation. Several NW-dipping fault planes display listric geometries. Vertical offsets vary between 3 and 35 cm. Like in the northern wall, faults which are oriented antitethically to the master fault dip more steeply than syntethic faults. In two places, planar conjugate faults are nearly symmetrical with respect to the bedding planes which are inclined with about 20° to the SE (Fig. 4). These faults presumedly formed in horizontally bedded strata and were rotated to their present orientation during rollover formation.

Finite extension by syntethic and antitethic faults has been computed for both walls of the pit. For the faults cropping out in the northern wall, horizontal extension parallel to the average fault dip direction (304°) sums up to 11.6 %. Syntethic NW-dipping faults account for 11.2 %, antitethic SE-dipping normal faults caused only 0.4 % horizontal extension. In the southern wall, syntethic faulting (0.7 %) and antitethic faulting (0.3 %) sum up to 1.0 % total extension. All values are thought to give maximum strain estimates as several faults do not offset the entire sequence. The estimates of finite extension clearly indicate that mesoscale antitethic normal faults were of very low importance during rollover formation and hangingwall collapse.

Fractured pebbles

In several middle- to coarse grained, clast-supported conglomerates pebbles display regular fractures and solution pits. Carbonate clasts show concave/convex grain contacts which are oriented subparallel to bedding and which are indicative for pressure solution along grain boundaries during compaction. Fractures measured in two stations dominantely strike NE to NNE, i.e., parallel to the exposed normal faults. Grain fabrics and microscale offsets allow to identify subvertical extension fractures and SE-dipping shear fractures which offset individual pebbles (Fig. 5). Fracture orientations and field observations (Fig. 5-1) show that subvertical fractures are more frequent than NW-dipping shear fractures. Dissolution pits and fractures indicate vertical shortening during compaction and subhorizontal extension paralleling the extension direction in the rollover. Strain geometry is coaxial plane strain.

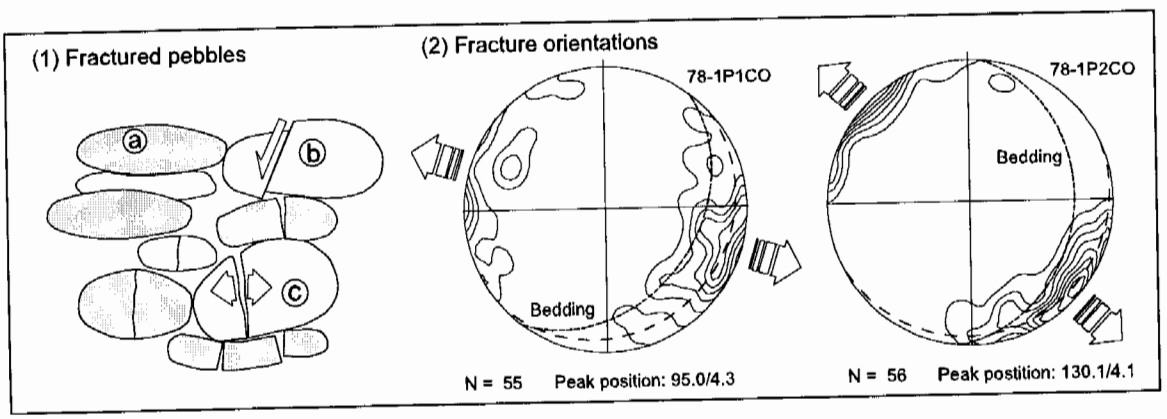

Fig. 5. (1) Small-scale deformational structures in pebbles of medium- to coarse grained, clast supported conglomerates. Sketches show cxonvex/concave grain boundaries due to (a) pressure solution of carbonate clasts, (b) extensional fractures and (c) shear fractures which were observed less frequently. (2) Orientations of fractures in pebbles measured in two conglomerate layers. Both subvertical tensile fractures and NW-dipping shear fractures are included in the diagram.

Discussion and conclusions

The mesoscale faults mapped in the St. Margatethen sandpit and the low finite strain estimated for these faults indicates that mesoscale faulting was only of minor importance during the formation of rollover adjacent to the eastern boundary fault of the Eisenstadt Basin. The only significant offsets were recorded for normal faults which dip syntethically to the listric master fault. Antitethic faults accomodated much less than 1 % extensional strain and, therefore, did not contribute to the evolution of the observed growth strata- and rollover geometry. If, at all, simple-shear deformation had a marked influence during hanging-wall collapse, distributed shear must have occured on a much smaller scale, at the scale of the grains of the deformed sediments. Observations in conglomerates of the rollover indicate that some deformation occured by pressure solution and fracturing of pebbles. Deformed pebbles indicate the predominance of coaxial pure-shear deformation related to compaction and extension parallel to the dip direction of normal faults. Although microscale shear fractures seem less important, additional simple-shear deformation by movement along grain boundaries cannot be excluded.

The hypothesis of distributed simple-shear deformation during hanging-wall collapse can be tested by comparing the observed geometries of early-formed conjugate normal faults which were rotated together with the bedding planes to deformation patterns which were modelled for vertical simple shear, antitethic simple shear and fault-bend folding. Fig. 6 shows geometrical models in which conjugate normal faults which formed prior to hanging-wall rollover were subjected to distributed simple-shear deformation.

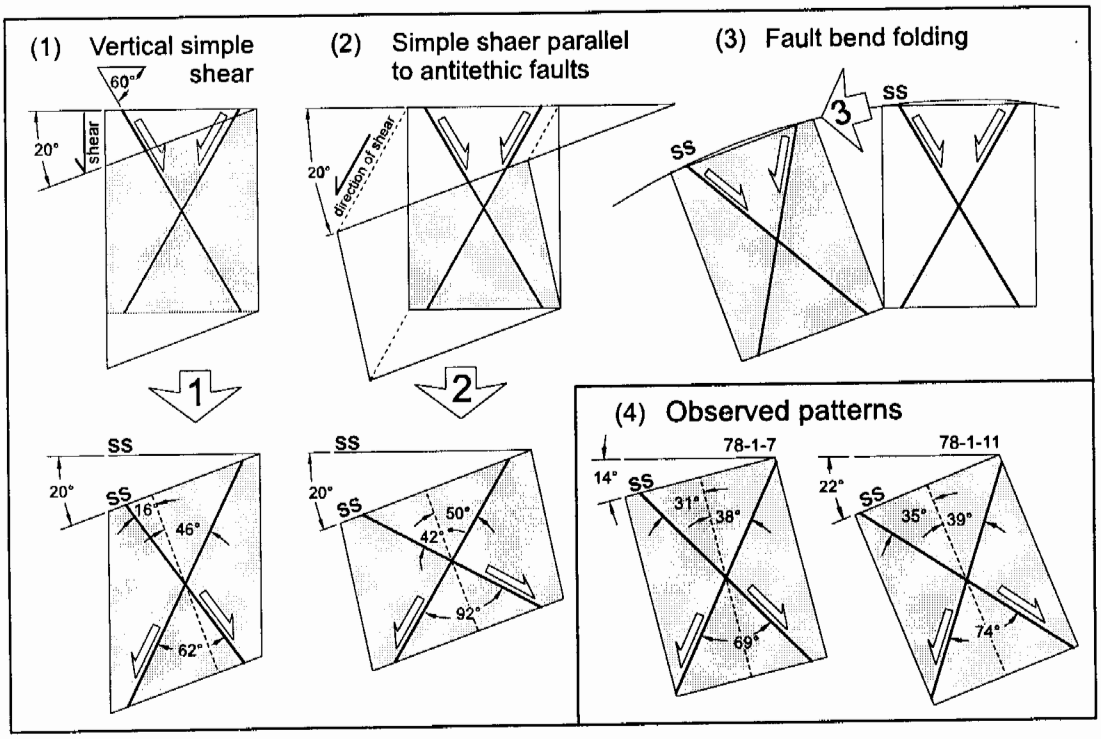

Fig. 6. Diagram illustrating distributed simple-shear deformation of conjugate normal faults which formed prior to rollover formation. The models for (1) vertical simple-shear and (2) simple-shear parallel to antitethic normal faults show that bedding planes, antitethic and syntethic faults are roteted for various degrees. Simple-shear was applied until bedding planes were rotated for 20° in order to compare the modelled geometries to (4) observed fault patterns. Fault orientations after vertical shear are strongly asymmetric with respect to bedding. Antitethic simple shear markedly increases the angle between conjugate faults. (3) Unlike the shear models, fault-bend folding conserves the relative orientations of faults and bedding planes. Note that both shear models do not match the observed fault patterns.

The models for vertical simple-shear and simple-shear parallel to antitethic normal faults show that bedding planes, antitethic and syntethic faults are rotated for various degrees. In both models, simple-shear was applied until bedding planes were rotated for 20° in order to compare the modelled geometries to observed conjugate faults depicted in Fig. 4. During vertical simple shear, antitethic and syntethic faults rotate to orientations which are strongly asymmetric with respect to the rotated bedding plane (Fig. 6-1). Sheared syntethic faults include lower angles (16°) with the plane normal to bedding than sheared antitethic faults (46°). The angle between the conjugate faults (originally 60°) does not change significantly. The resulting pattern strongly contrasts from the pattern acchieved by antitethic shear (Fig. 6-2). During antitethic shear, faults which parallel the direction of shearing are not rotated. The resulting pattern of deformed conjugate faults is nearly symmetrical to bedding with faults including 42° and 50° with the plane normal to bedding. This pattern and the high angle between the conjugate faults (92°) clearly distinguishes antitethic- from vertical shear deformation.

Comparison of the modelled geometries to the patterns observed in the sandpit (Fig. 4; Fig. 6-4) shows that the observed patterns are distinct from the geometries predicted for both vertical and antitethic simple shear. The conjugate faults which were mapped in beds dipping with 14° and 22° to the SE include about 70° with each other and are only slightly asymmetric with respect to bedding. Distributed shear required for the observed tilting of beds should lead to more asymmetric patterns in the case of vertical shear. In the case of antitethic shear, the angle between the conjugate faults should have increased markedly. The observed patterns can, however, be explaned by block rotation during fault-bend folding which conserves the relative orientations of bedding planes and normal faults.

Acknowledgements

K. D. greatfully acknowledges financial supported by the Austrian Project of Advanced Research and Technology of the Austrian Academy of Sciences and by the Austrian Science Foundation (Project P 10683 GEO). Both authors thank the OMV for supporting structural research in Austria's Neogene basins. The working permission by the owner of the sandpit, Eduard Kaufer, is greatfully acknowledged. We thank Peter Pervesler, Reinhard Rötzel and all other participants of the SS '96 paleontology field course for logistical support and Günther Pascher for his excellent Geo-Wine '95 which rewarded us for agressive field work.

References

Ellis, P.G. and McClay, K.R., 1988. Listric extensional fault systems - results of analogue model experiments. Basin Res., 1: 55-70.

Fuchs, W., 1965. Geologie des Ruster Berglandes (Burgenland). Jb.Geol. B.-A., 108: 1565-194.

Groshong, R.H., jr., 1989. Half-graben structures: Balanced models of extensional fault-bend folds. Geol.Soc.Am.Bull., 101(1): 96-105.

Hermann, P., Pascher, G. and Pistotnik, J., 1993. Geologische Karte der Republik Österreich 1:50.000, Blatt 78 Rust (7812). Geol. B.-A., Wien.

Kröll, A. and Wessely, G., 1993. Wiener Becken und angrenzende Gebiete - Strukturkarte-Basis der tertiären Beckenfüllung. Geologische Themenkarte der Republik Österreich 1:200.000.

Lueger, J., 1980. Die Molluskenfauna aus dem Pannon (Obermiozän) des Fölligberges (Eisenstädter Bucht) im Burgenland (Österreich). Mitt.österr.Geol.Ges., 73: 95-134.

Piller, W.E., Decker, K. and Haas, M., 1996. Sedimentologie und Beckendynamik des Wiener Beckens. Ber. Geol. B.-A., 33: 41pp.

Piller, W.P. and Vávra, N., 1991. Das Tertiär im Wiener und Eisenstädter Becken. In: Roetzl, R.and Nagel, D. (Eds.). Exkursionen im Tertiär Österreichs, Molassezone - Waschbergzone - Korneuburger Becken - Wiener Becken - Eisenstädter Becken, 169-216.

Rowan, M.G. and Kligfield, R., 1989. Cross section restoration and balancing as aid to seismic interpretation in extensional terranes. Am.Assoc.Petrol.Geol., Bull., 73(8): 955-966.

Tollmann, A., 1955. Das Neogen am Nordwestrand der Eisenstädter Bucht. Wiss. Arb. Burgenland, 10: 1-74.

Tollmann, A., 1985. Das Eisenstädter Becken. In: Tollmann, A. (Ed.), Geologie von Österreich, Band 2, Deuticke, Wien, 532-544.

Wessely, G., 1993. Geologischer Tiefbau Wiener Becken - Molasse Niederösterreichs. In: Brix, F. and Schulz, O. (Eds.). Erdöl und Erdgas in Österreich, Wien, Beil.

White, N.J., Jackson, J.A. and McKenzie, D.P., 1986. The relationship between the geometry of normal faults and that of the sedimentary layers in their hanging walls. J.Struct.Geol., 8(8): 897-909.

White, N. and Yielding, G., 1991. Calculating normal fault geometries at depth: theory and examples. In: Roberts, A.M., Yielding, G. and Freeman, B. (Eds.). The Geometry of Normal Faults. Geol.Soc.London Spec.Publ., 56, 251-260.

Xiao, H. and Suppe, J., 1989. Role of compaction in the listric shape of growth normal faults. Am.Assoc.Petrol.Geol., Bull., 73: 777-786.